

First Observation of an X-Ray Beam Following a New Geodesic When Gravitational Waves Deform Space-Time

Edward Jiménez¹, Nicolás Recalde², Wilson P. Álvarez-Samaniego³, Borys Álvarez-Samaniego³, Douglas Moya-Álvarez³ & Esteban Jiménez⁴

¹ Department of Chemical Engineering, Universidad Central del Ecuador (UCE), Quito, Ecuador

² Department of Physics and Astronomy, University of South Carolina, USA

³ Núcleo de Investigadores Científicos, Universidad Central del Ecuador (UCE), Quito, Ecuador

⁴ Sciences Technologie et Santé, Université Toulouse III-Paul Sabatier, France

Correspondence: Edward Jiménez, Gerónimo Leiton S/N y Gatto Sobral, Department of Chemical Engineering, Universidad Central del Ecuador (UCE), 170521 Quito, Ecuador. E-mail: ehjimenez@uce.edu.ec

Received: January 6, 2019 Accepted: February 26, 2019 Online Published: March 1, 2019

doi:10.5539/jmr.v11n2p53

URL: <https://doi.org/10.5539/jmr.v11n2p53>

Abstract

By using X-rays of a linear accelerator (LINAC Siemens X rays, 6 MeV) for medical use, we were able to measure gravitational waves, GW, (amplitude = 56.385mm , frequency = $1/3\text{Hz}$, velocity = c and polarization) and its three-dimensional effect on X-ray trajectories. The collimated X-ray beam, which is in the plane (X, Y) , travels on the Z axis at the speed of light in air and passing through the machine isocenter, until it reaches the target and, ultimately, is recorded in a radiographic film. Apparently, there is an exceptional coincidence in the operation of LINAC and the presence of GW. This coincidence occurred in VIRGINIA, GPS (38.634 351 1, -77.282 523 9), UTC (12/06/2011: 12: 56: 01). This important event, but not sui generis, was recorded in the LINAC computer system, on a film for radiography, in the log file of the cancer treatment center and it was reported to SIEMENS in order to try to find an explanation of a possible hardware failure, some abnormality or any software issue. The physicist and Siemens service engineer on site concluded that such event should never happen because LINAC was not malfunctioning. Consequently, for the X-rays, there was a deviation of the isocenter of the LINAC ($\Delta X = (11.5 \pm 0.5)\text{mm}$, $\Delta Y = (48 \pm 0.5)\text{mm}$), by the action of the amplitude of GW. The tolerance of a LINAC is lower than these measurements, and the equipment will stop working if they are greater than $\pm 1.0\text{mm}$ for isocenter (zero position) and $\pm 2.0\text{mm}$ for other collimator leaf positions. Therefore, this constitutes a register of space-time alteration with a consequent variation of the path of the X-ray beam. Finally, the registered gravitational waves leave invariant the angle between the axes (X, Y) , of the X-ray beam, indicating a constant polarization.

Keywords: X-ray beam, isocenter, geodesic, gravitational waves

1. Introduction

The detection of gravitational waves, GW, is a collaborative achievement of this century, and it will mark the new challenges of astrophysics and future astronomy (Abbott, B. P. et al., February 2016, June 2016). Emblematic projects such as LIGO and VIRGO are examples of the new way that the scientific community is working, (Abbott, B. P. et al., 2018, 2018 A, 2018 C), where some questions are resolved in a multidisciplinary way, not only in the philosophical conception or the methodology of research, but also, about the use of equipment and infrastructure that modern society and technology have at their disposal, including: nanotechnology embedded in hardware and software devices in cancer treatment equipment (Xoft, LINAC), low energy X-ray spectroscopy, X-ray telescopes (Chandra, Hitomi, Newton), nuclear magnetic resonance in Quantum Computation, catalysis and plasma in petroleum refining, among others (Abbott, B. P. et al., June 2017, October 2017), (Piasetzky, Sargsian, Frankfurt, Strikman and Watson, 2006).

The precision of the LIGO experiments (Livingston, Hanford) constitutes an international reference in laser light interference in gravitational waves detection (Ciufolini, 2007), (Álvarez-Samaniego, W. P., Álvarez-Samaniego, B. and Moya-Álvarez, 2017), (Hawking and Israel (Eds.), 1979), with the following characteristics:

1. Interferometric laser system with two perpendicular arms under vacuum conditions together with an optical path of 4Km in Livingston and 2Km in Hanford. It is based on detecting gravitational waves through tiny movements they produce in mirrors, which results in the generation of a diffraction pattern in the interferometer signal.
2. GW originating millions of light years from Earth distort the surfaces of mirrors in interferometers about 10^{-18}m (the proton has a size of $0.843 \times 10^{-15}\text{m}$) (Abbott, B. P. et al., February 2016, 2018, 2018 A).

3. The duplication of readings from two different observatories allows us to identify false detections produced by local effects such as small seismic disturbances or an instruments failure.

4. The construction of Advanced LIGO was completed in February 2015 and its scientific mission began in September of that year, with a sensitivity four times greater than the initial design.

The fundamental fact about LIGO detection is about the space-time-matter interaction, which appears as a single entity. This last can be explained later on this paper making use of the linearization of Einstein’s equations.

Therefore, after establishing the LIGO the basic elements of the measurement technique, we can formulate the question below:

Is it possible to study GW through the alteration of the trajectory of an X-ray beam in the deformed space-time? The answer is yes, in

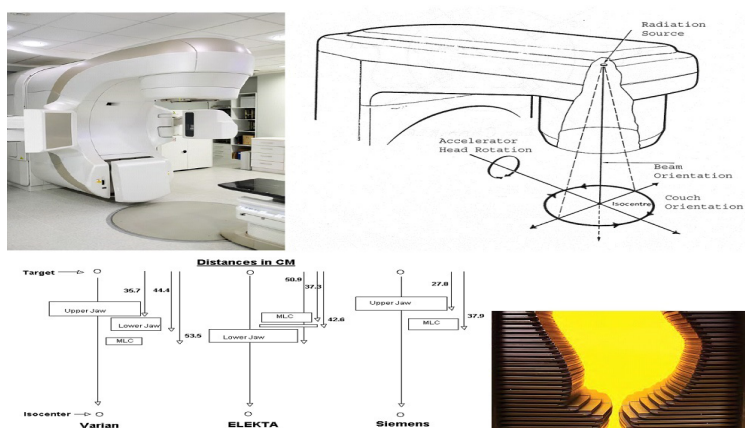


Figure 1. LINAC Siemens elements

light of the following premises or requirements:

1. We need to use a high-energy X-ray beam, to ensure that it travels at the speed of light in a vacuum, because its cross-section depends inversely on the energy (Rowshanfarzad, Sabet, O’Connor and Greer, 2011), (Litzenberg, Gallagher, Masi, Lee, Prisciandaro, Hamstra, Ritter and Lam, 2013).
2. We must establish a beam of X-rays, having a defined shape and with a reference system attached to the beam.
3. We must measure the interaction of the gravitational wave with the X-ray beam, to determine amplitude, frequency and polarization.
4. We must know the trajectory of the X-rays before the passage of the gravitational wave, in order to establish comparisons and differences in the space-time tissue.

The unique technology that meets all these requirements is already implemented around the world for the treatment of cancer and it is called LINAC (Rowshanfarzad et al., 2011), (Sontag and Steinberg, 1999). In order to measure GW, we simply take the data from a functioning LINAC, during the passage of a gravitational wave.

2. Equipment and Materials: Linear Accelerator

Figure 1. LINAC Siemens elements. In the upper left figure, we can see the appearance of the LINAC Siemens, with a strong robustness and a weight of the order of tons. The upper right figure indicates the main elements of the LINAC head where X-ray radiation is produced and considered an X-ray source, collimation and multi leaf collimator (MLC) systems. The isocenter is the reference point for mechanical and radiation field which has a maximum tolerance

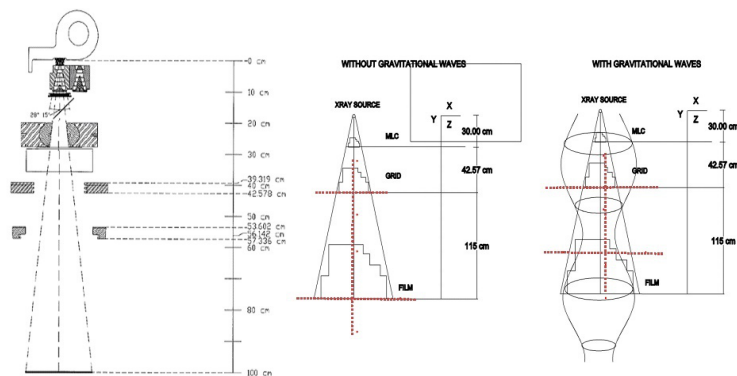


Figure 2. 3-D Radiation Beam Path through MLC or OPTIFOCUS MLC EQUIPPED Digital Linear Accelerator

of $\pm 1mm$. The lower left figure indicates the distances between the Upper Jaw and the MLC, for some LINAC's. Finally, the lower right figure indicates 80 leaves of the MLC, which produces the shape of the X-ray beam. This last also corresponds to the shape of the target. Each MLC leaf is calibrated by an independent system that has a maximum tolerance of $\pm 2mm$.

2.1 LINAC. SIEMENS PRIMUS 6 MV X Rays

We will specify its important parts for the development of this experiment.

X-ray source

It is a source of X-rays, with an energy of 6 MeV, located in the position $Z = 0$. X-rays from this point will pass through the collimators and then through the patient's tumor or target and finally being recorded in a FILM.

MultiLeaf collimator (80 leafs)

The X bank contains the 80 sheets of the MLC and is 19.685cm from the X-ray source. The MLC bank is located below the Y-jaws bank.

Y-jaws bank consists of two thick tungsten leaves located above the MLC.

The isocenter reference grid is installed at 42.578cm.

Radiography X-ray film is placed after target and It is perpendicular to radiation beam passing through LINAC's isocenter.

It is an exploratory technique that consists of subjecting a body or an object to the action of X-rays to obtain an image on a photographic plate. Image or photograph is obtained by means of this exploratory technique. Minimum irradiation time is 3s in order to obtain a good resolution and according to film's response curve.

Figure 2. 3-D Radiation Beam Path through MLC or OPTIFOCUS MLC EQUIPPED Digital Linear Accelerator. The interaction or perturbation measured by the action of GW occurs in the section between the MLC collimator located at $Z = 19.685cm$ and the isocenter grid located at $Z = 42.578cm$. Of course, the gravitational wave also affects the trajectory from the MLC to the FILM and uniformly throughout the beam path. The figure of the center indicates the collimator, the isocenter and the X-ray beam without the presence of GW. While the figure on the right takes into account the presence of GW, where we it is possible to see how the displacement of the isocenter occurs.

3. Method

EQUIPMENT:

LINAC. SIEMENS PRIMUS 6 MV X RAYS.

PLACE:

POTOMAC RADIATION ONCOLOGY CENTER:

Virginia. (38.634 351 1, -77.282 523 9).

DATE & TIME:

12/06/2011 FROM 8:56 TO 8:57

GREENWICH MEAN TIME (UTC): 12/06/2011 FROM 12:56 TO 12:57.

TOLERANCE LIMITS:

$\pm 1.0mm$ for isocenter (zero position) & $\pm 2.0mm$ for other leaf positions.

DATES OF VERIFICACION DATA.

12/06/2011, 12/07/2011, 12/07/2011.

We will explain why the presence of GW in the Earth is not an exaggeratedly improbable phenomenon, but rather it can be detected by linear accelerators that are used to treat cancer.

1. In the LINAC Gantry, the X-ray source, the Isocenter, the primary and secondary collimators are physically located, controlled and well defined.
2. Source of X-rays, is located in the upper part of the LINAC head.
3. The isocenter is unique, defined, constructed and operated in an exact manner from the start to the end of the lifespan of the LINAC.
4. Bank of tungsten collimators X and Y , which have an autonomous control system for each leaf. The geometric figure formed in the MLC will represent the shape of the tumor to be irradiated.
5. Regarding the machine mechanical Isocenter, it has an accuracy less than $1mm$ with a tolerance of $\pm 1mm$.
6. X-ray recording FILM. It is located after the target at a distance of $115cm$ from the source of X-rays and perpendicular to the X-ray beam axis. The X-rays will travel through isocenter and target and ultimate are registered on a photographic film.

3.1 Functioning of the LINAC and Interoperability of Its Parts

3.1.1 Measurement of Amplitude, Frequency and Polarization of the Gravitational Wave

The gravitational wave is characterized by: amplitude, frequency, polarization and speed. It is a phenomenon that alters space-time and travels at the speed of light in the vacuum. When a beam of X-rays fully defined in shape and size passes through the modified space-time, it undergoes a modification in shape and size. From this gravitational wave we can measure and/or calculate amplitude, frequency and polarization.

The amplitude is measured through the displacements in the trajectory of the X-rays and it is equal to $\Delta X = (11.5 \pm 0.5)mm$ and $\Delta Y = (48 \pm 0.5)mm$.

The frequency of the gravitational wave is measured indirectly by the response curve of the irradiated film. This last is true since in order to obtain an adequate contrast on film a minimum of 3s of irradiation is needed, so that the frequency is equal to $\nu = 1/3Hz$. This result agrees with the theoretical studies (Hawking and Israel, 1979) that establish that frequency of GW must be in the interval $[10^{-7}, 10^{11}]Hz$.

Polarization: Plus-polarized, Cross-polarized

X-ray beam in reference to the Isocenter. The irradiated tumor has an identical shape previously defined, modeled and constructed in the MLC.

It is a figure whose shape is given by tungsten collimators and Y-jaws. It has a defined isocenter and fully calibrated and verified every day before starting operation in any cancer treatment center, in particular, POTOMAC-RADIATION-CENTER.

Triple control systems

- The linear accelerator used to treat cancer is triple controlled by three independent systems to guarantee the dose given to the patient and delivered to the exact area or tumor volume. The LINAC have an accuracy less than $1mm$ and a tolerance of maximum $\pm 1mm$.
- The irradiation process will start only when the calibration of the area to be irradiated is correct and checked by the LINAC systems.
- If one of the systems that control the MLC is not in perfect alignment with the reference system or isocenter, then the LINAC automatically stops its operation until a non-perfect alignment is corrected.
- The X-rays were properly recorded on the film showing a displacement in X and Y . This was not detected by any of the

systems that control any signs of no alignment or displacement. The only possibility for this phenomenon to occur can be understood if we consider that something moved, at the speed of light in the vacuum, and disturbed the space-time of the X-ray beam.

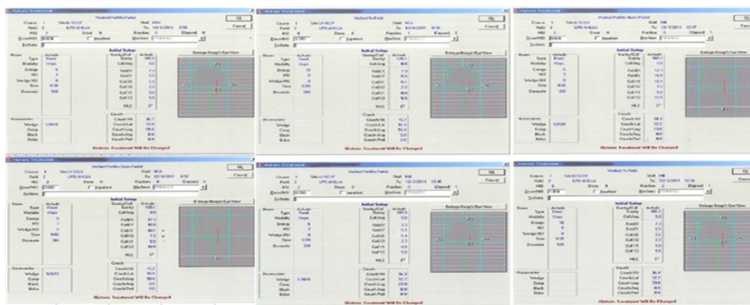


Figure 3. First control system for a correct functioning of the LINAC

4. Results

The X-rays came out of the source, crossed the collimator, crossed the tumor and arrived at the FILM, demonstrating that the isocenter and the equipment are properly calibrated and work perfectly.

On the radiographic film, we can see that the isocenter is displaced by X and it is recorded. We measure the displacements and obtain a distance for $\Delta X = (11.5 \pm 0.5) \text{ mm}$, and for $\Delta Y = (48 \pm 0.5) \text{ mm}$.

The source, the isocenter, the collimator, the FILM are aligned on the Z axis.

The X-rays traveled at the speed of light, c , a length $L = (1150 \pm 10) \text{ mm}$ at a time $t = \frac{L}{c} \approx \frac{1.15}{c} \text{ s}$, while the possible gravitational wave traveled at the speed of light the distance: $(\Delta X^2 + \Delta Y^2)^{1/2}$.

Isocenter displacement

Displacement in $x = 11.5 \text{ mm} \pm 0.5 \text{ mm}$.

Displacement in $y = 48 \text{ mm} \pm 0.5 \text{ mm}$.

The gravitational wave must have constant polarization.

Figure 3. First control system for a correct functioning of the LINAC. Hours and records are indicated in LINAC report and dated 12/06/2011 in Washington, D.C. The figures correspond to records of gravitational abnormality, which indicate total normality between the radiation field of the LINAC and the Isocenter, where no displacement in X nor in Y is observed. This was verified, minute by minute throughout of the working day in the laboratory, without observing any abnormality in the primary control system and having the values of 8:56, NORMAL; 8:57, NORMAL; 8:58, NORMAL; 10:46, NORMAL; 10:54, NORMAL.

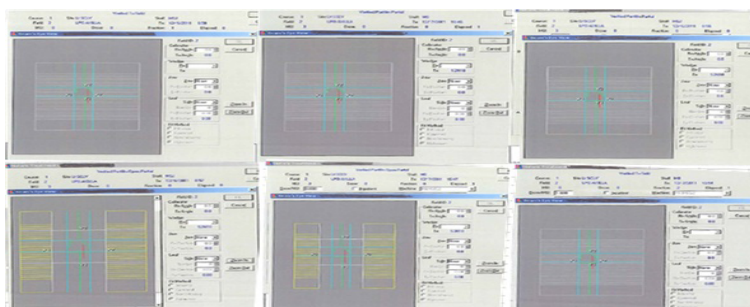


Figure 4. Second control system for a correct functioning of the LINAC

According to Figure 3, it is concluded that the disturbance occurs after X-ray source emitted photons at the time: 12/06/2011: (08:56:01) Washington, D.C. time, (UTC: 12/06/2011 FROM 12:56:01 TO 12:56:03).

Figure 4. Second control system for a correct functioning of the LINAC. This second redundant control system indicates that the LINAC is working perfectly previous to the irradiation of the patients and explicitly on 12/06/2011 at (08:56:00) Washington, D.C. time. After this second verification the LINAC starts the X-ray irradiation to the patient.

Figure 5. We can observe in the film the variation of the isocenter of the X-ray beam, with respect to the X and Y coordinates. The upper figures indicate the isocenter placement before and after the passage of the gravitational wave. The lower figures indicate the displacement of the isocenter during the passage of the gravitational wave.

5. Discussion of Results

We have shown that there was no instrumental error when taking the film (radiography) and therefore, the disturbance on film registration is due to the passage of a gravitational wave, which altered the space-time trajectory of the X-ray photons.



Figure 5. The film variation of the isocenter of the X-ray beam

5.1 The 80 Leaves Collimator Motion

The collimator system defines the shape of the tumor has an autonomous control together with an independent system that drives each leaf. It is a mechanical device that works at speeds supremely lower than the speed of light ($v/c = 92.5925 \times 10^{-9}$) and it could never be relocated to define a new isocenter in less than $1/3 \times 10^{-9} ns$, which was the time of duration of the phenomenon.

Electromechanical impossibility.

5.2 The Isocenter Motion

The isocenter is built and verified during the installation of the linear accelerator LINAC and it has three control subsystems, before carrying out an X-ray irradiation. When the LINAC is out of calibration or defective, these control subsystems stop the LINAC operation and simply does not irradiate.

During the dates of the gravitational phenomenon, (12/06/2011, 12/07/2011, 12/07/2011), no anomaly was reported. However, due to the strange information recorded on film, the correct functioning was checked and the company SIEMENS was contacted to evaluate some type of abnormality in the equipment. No abnormality was detected. All the analysis work was duly recorded by the oncologist and the chief physicist.

Impossibility of a new isocenter or double isocenter.

5.3 Theoretical Implications

The gravitational waves interacting with our planet Earth, do so at non-relativistic speeds, allowing the coupling of matter with space-time, creating a new fully coupled system that we call *space-time-matter*. This space-time-matter system obeys a coupled system of partial differential equations called *Linearized Einstein's field equations* (see (Álvarez-Samaniego, W. P. et al., 2017)). This system can be obtained from the Einstein field equations, as an approximation of weak fields and for speeds much lower than the speed of light in vacuum (see (Álvarez-Samaniego, W. P. et al., 2017)). It is also shown in (Álvarez-Samaniego, W. P. et al., 2017) that there is an additional term for the *space-time-mass density* that corresponds to the curvature of space-time. According to the LIGO experiment, the gravitational waves originating on reaching the Earth distort the surfaces of the mirrors in the interferometers by $10^{-18} m$. This phenomenon has not been explained yet, nor it

is understood how this interaction with the mirrors takes place. However, the physical explanation and the mathematical proof, given in (Álvarez-Samaniego, W. P. et al., 2017), shows the existence of a space-time-matter coupling, given by the following system

$$\left\{ \begin{aligned} \nabla \times \vec{E}_g &= -\frac{1}{c} \frac{\partial \vec{B}_g}{\partial t}, & (1.1) \\ \nabla \cdot \vec{E}_g &\approx -4\pi G \rho_g, & (1.2) \\ \nabla \times \vec{B}_g &\approx -\frac{4\pi G}{c^2} \vec{J}_g + \frac{1}{c} \frac{\partial \vec{E}_g}{\partial t}, & (1.3) \\ \nabla \cdot \vec{B}_g &= 0, & (1.4) \end{aligned} \right.$$

where $\vec{E}_g = \vec{E}_g(m, x, y, z, t)$ is the *gravitoelectric field*, $\vec{B}_g = \vec{B}_g(m, x, y, z, t)$ is the *gravitomagnetic field*, $\vec{J}_g = \vec{J}_g(m, x, y, z, t)$ is the *space-time-mass current density* and $\rho_g = \rho_g(m, x, y, z, t)$ is the *space-time-mass density*. The gravitoelectromagnetic field system (1.1)-(1.4) is equivalent to the Maxwell equations in a suitable approximation, thus showing a good analogy between the classical electromagnetic theory and Einstein's gravitational theory. Through this similarity, it is possible to establish a model for the quantization of gravity.

6. Conclusions

1. The detection of GW is a very common experiment of daily life. It may affect cancer treatments and any device that uses ionizing radiation. Especially, it may alter particles that travel at speeds close to the light in a vacuum.
2. The only way to measure the amplitude of a gravitational wave is that simultaneously such a wave affects a conglomerate of photons (X-rays) in three dimensions, that is, in the polarization axes and in the propagation direction of the gravitational wave.
3. The GW deform the space-time and a sufficient period of time (3s) is needed for X-rays to pass through this deformation and undergo changes in the measurements of time and/or space. It became necessary to analyze a whole beam of X-rays, which form a closed surface of dimensions recorded in Figures 3, 4 and 5. From experiment characteristics and, mainly due to a space fixed mechanical isocenter, we were able to record on a film that indeed isocenter could largely move under the action of a gravitational wave.
4. Future experiments may measure other properties of GW. For example, geostationary satellites dedicated to the monitoring of GW. They will measure every second the travel time of laser light between geostationary satellites and fixed points of the earth. This could be possible for a minimum number of satellites, in such a way that the terrestrial surface is covered and, space-time variations can be inferred by the passage of GW.
5. Experiments with high-energy X-rays are convenient, due to their very small interaction cross-section which is in the range of femtometers. This guarantees that they travel at the speed of light in the vacuum and they can interact with GW in a direct way. The physical variables can be fully measurable, due to technological advances on cancer treatment devices, using x-rays.
6. The detection of GW is now a very common experiment of daily life, and it may affect cancer treatments and any device that uses ionizing radiation. Especially, it may disturb particles that travel at speeds close to the light in the vacuum.
7. The only way to measure the amplitude of a gravitational wave is when it simultaneously perturbs a conglomerate of photons (X-rays) in the three dimensional space. That is to say, in the polarization axes and along the direction of propagation of the gravitational wave.
8. In agreement with the scientific method, several possible causes of this space-time disturbance were analyzed, discarding a possible tectonic phenomena and some atypical astronomical event different from GW. It is sufficient to review the following pages to support the last assertion. Moreover, the equipment, used in this experiment that was installed for cancer treatment around the world (LINAC Siemens), does not work when there are tectonic, volcanic or electromagnetic phenomena that may alter the measurements and the treatment dose. Hence, it is not possible to think that any cause of this nature might have affected this experiment.

Acknowledgments

To the faculty and students of the Department of Chemical Engineering of Universidad Central del Ecuador. To the participants of the 3rd. Edition of International Conference on Advanced Spectroscopy, Crystallography and Applications in Modern Chemistry during June 04-05, 2018, London, UK. To the participants of the congress CIPANP 2018 - Thirteenth

Conference on the Intersections of Particle and Nuclear Physics, from May 29 to June 03, 2018, Berkeley, USA.

References

- Abbott, B. P. et al. (LIGO Scientific Collaboration and Virgo Collaboration). (February 2016). Observation of gravitational waves from a binary black hole merger. *Physical Review Letters*, 116(6), 061102.
- Abbott, B. P. et al. (LIGO Scientific Collaboration and Virgo Collaboration). (June 2016). GW151226: Observation of gravitational waves from a 22-solar-mass binary black hole coalescence. *Physical Review Letters*, 116(24), 241103.
- Abbott, B. P. et al. (LIGO Scientific Collaboration and Virgo Collaboration). (June 2017). GW170104: Observation of a 50-solar-mass binary black hole coalescence at redshift 0.2. *Physical Review Letters*, 118(22), 221101.
- Abbott, B. P. et al. (LIGO Scientific Collaboration and Virgo Collaboration). (October 2017). GW170817: Observation of gravitational waves from a binary neutron star inspiral. *Physical Review Letters*, 119(16), 161101.
- Abbott, B. P. et al. (LIGO Scientific Collaboration and Virgo Collaboration). (December 2017). GW170608: Observation of a 19-solar-mass binary black hole coalescence. *The Astrophysical Journal Letters*, 851(2), L35.
- Abbott, B. P. et al. (LIGO Scientific Collaboration and Virgo Collaboration). (2018). Search for tensor, vector, and scalar polarizations in the stochastic gravitational-wave background. *Physical Review Letters*, 120(20), 201102.
- Abbott, B. P. et al. (LIGO Scientific Collaboration and Virgo Collaboration). (2018 A). Full band all-sky search for periodic gravitational waves in the O1 LIGO data. *Physical Review D*, 97(10), 102003.
- Abbott, B. P. et al. (LIGO Scientific Collaboration and Virgo Collaboration). (2018 C). GW170817: Constraints on cosmic strings using data from the first advanced LIGO observing run. *Physical Review D*, 97(10), 102002.
- Álvarez-Samaniego, W. P., Álvarez-Samaniego, B., & Moya-Álvarez, D. (2017). Linearized Einstein's field equations. *Matemática: Una publicación de FCNM-ESPOL*, 15(2), 48-55. <https://arxiv.org/abs/1710.01593>
- Ciufolini, I. (2007). Dragging of inertial frames. *Nature*, 449(7158), 41-47.
- General Relativity: An Einstein Centenary Survey. (1979). Edited by Hawking, S. W., & Israel, W. Cambridge, UK: Cambridge University Press.
- Litzenberg, D. W., Gallagher, I., Masi, K. J., Lee, C., Prisciandaro, J. I., Hamstra, D. A., Ritter, T., & Lam, K. L. (2013). A measurement technique to determine the calibration accuracy of an electromagnetic tracking system to radiation isocenter. *Medical Physics*, 40(8), 081711.
- Piassetzky, E., Sargsian, M., Frankfurt, L., Strikman, M., & Watson, J. W. (2006). Evidence for strong dominance of proton-neutron correlations in nuclei. *Physical Review Letters*, 97(16), 162504.
- Rowshanfarzad, P., Sabet, M., O'Connor, D. J., & Greer, P. B. (2011). Isocenter verification for LINAC-based stereotactic radiation therapy: review of principles and techniques. *Journal of Applied Clinical Medical Physics*, 12(4), 3645.
- Sontag, M. R., & Steinberg, T. H. (1999). Performance and beam characteristics of the Siemens Primus linear accelerator. *Medical Physics*, 26(5), 734-736. <https://doi.org/10.1118/1.598580>

Appendix A

Figure 1. LINAC Siemens elements. In the upper left figure, we can see the appearance of the LINAC Siemens, with a strong robustness and a weight of the order of tons. The upper right figure indicates the main elements of the LINAC head where X-ray radiation is produced and considered an X-ray source, collimation and multi leaf collimator (MLC) systems. The isocenter is the reference point for mechanical and radiation field which has a maximum tolerance of $\pm 1\text{mm}$. The lower left figure indicates the distances between the Upper Jaw and the MLC, for some LINAC's. Finally, the lower right figure indicates 80 leaves of the MLC, which produces the shape of the X-ray beam. This last also corresponds to the shape of the target. Each MLC leaf is calibrated by an independent system that has a maximum tolerance of $\pm 2\text{mm}$.

Figure 2. 3-D Radiation Beam Path through MLC or OPTIFOCUS MLC EQUIPPED Digital Linear Accelerator. The interaction or perturbation measured by the action of gravitational waves occurs in the section between the MLC collimator located at $Z = 19.685\text{cm}$ and the isocenter grid located at $Z = 42.578\text{cm}$. Of course, the gravitational wave also affects the trajectory from the MLC to the FILM and uniformly throughout the beam path. The figure of the center indicates the collimator, the isocenter and the X-ray beam without the presence of gravitational waves. While the figure on the right takes into account the presence of gravitational waves, where we can see how the displacement of the isocenter occurs.

Figure 3. First control system for a correct functioning of the LINAC. Hours and records are indicated in LINAC report and dated at Washington, D.C., December 06, 2011. The figures correspond to records of gravitational abnormality, which

indicate total normality between the radiation field of the LINAC and the Isocenter, where no displacement in X nor in Y is observed. This was verified, minute by minute throughout of the working day in the laboratory, without observing any abnormality in the primary control system and, having the values of 8:56, NORMAL; 8:57, NORMAL; 8:58, NORMAL; 10:46, NORMAL; 10:54, NORMAL.

Figure 4. Second control system for a correct functioning of the LINAC. This second redundant control system indicates that the LINAC is working perfectly previous to the irradiation of the patients and explicitly on December 06, 2011 at (08:56:00) Washington, D.C. time. After this second verification the LINAC starts the X-ray irradiation to the patient.

Figure 5. We can observe in the film the variation of the isocenter of the X-ray beam, with respect to the X and Y coordinates. The left figure indicates the isocenter placement before and after the passage of the gravitational wave. The right figure indicates the displacement of the isocenter during the passage of the gravitational wave.

Appendix B

Non-relativistic approximation of a weak gravitational field

- Using the classical theory of Newton and the existence of gravitational waves, we can obtain (see (Álvarez-Samaniego, W. P. et al., 2017)) the following system of classical equations for the *Newtonian gravitoelectric field*, \vec{g} , and the *gravitomagnetic field*, \vec{B}_g :

$$\begin{cases} \nabla \cdot \vec{g} &= -4\pi G\rho, \\ \nabla \times \vec{B}_g &= -\frac{4\pi G}{c^2} \vec{J} + \frac{1}{c^2} \partial_t \vec{g}, \\ \nabla \times \vec{g} &= -\partial_t \vec{B}_g, \\ \nabla \cdot \vec{B}_g &= 0, \end{cases} \tag{1}$$

where G is the *Cavendish gravitational constant*, ρ is the *mass density* and \vec{J} is the *current mass density*.

- On the other hand, the Einstein field equations are given by

$$R^{ik} - \frac{1}{2} g^{ik} R = \frac{8\pi G}{c^4} T^{ik}, \tag{2}$$

where for all $i, k \in \{0, 1, 2, 3\}$, R^{ik} are the contravariant components of the *Ricci tensor*, g^{ik} are the contravariant components of the *metric tensor*, T^{ik} are the contravariant components of the *energy-momentum tensor*, R is the scalar curvature and c is the *speed of light in vacuum*. Using (2) and the approximation for weak non-relativistic fields, we obtain the following system of equations (see (Álvarez-Samaniego, W. P. et al., 2017) for a complete proof):

$$\begin{cases} \nabla \times \vec{E}_g &= -\frac{1}{c} \frac{\partial \vec{B}_g}{\partial t}, \\ \nabla \cdot \vec{E}_g &\approx -4\pi G\rho_g, \\ \nabla \times \vec{B}_g &\approx -\frac{4\pi G}{c^2} \vec{J}_g + \frac{1}{c} \frac{\partial \vec{E}_g}{\partial t}, \\ \nabla \cdot \vec{B}_g &= 0, \end{cases} \tag{3}$$

where $\vec{E}_g \approx \frac{\vec{g}}{c}$ is the *gravitoelectric field*, \vec{B}_g is the *gravitomagnetic field*, $\rho_g := \frac{\rho}{c} - \frac{1}{4\pi c G} \frac{\partial E_g^0}{\partial t}$ is the *space-time-mass density* and \vec{J}_g is the *space-time-mass current density*. We can notice that in the approximation of the non-relativistic weak field, the density ρ_g is written as a multiple of the classical mass density ρ plus a term corresponding to the curvature of space-time, proportional to $\frac{\partial E_g^0}{\partial t}$, which constitutes a relativistic correction to the Newtonian classical system, given by (1). Using the last system of equations (3), and considering empty space and weak gravitational fields, it is possible to obtain (see (Álvarez-Samaniego, W. P. et al., 2017)) the following hyperbolic equations for the fields \vec{E}_g and \vec{B}_g :

$$\Delta \vec{E}_g \approx \frac{1}{c^2} \frac{\partial^2 \vec{E}_g}{\partial t^2} \tag{4}$$

and

$$\Delta \vec{B}_g \approx \frac{1}{c^2} \frac{\partial^2 \vec{B}_g}{\partial t^2}. \quad (5)$$

Equations (4) and (5) above prove the existence of gravitational waves even in the non-relativistic approximation for weak fields. Moreover, considering empty space and weak gravitational fields, one has that $\rho_g = -\frac{1}{4\pi cG} \frac{\partial E_g^0}{\partial t}$, even though no mass is present. Here, $\frac{\partial E_g^0}{\partial t}$ corresponds to the contribution made by the curvature of space-time, which has no classical analogy.

Copyrights

Copyright for this article is retained by the author(s), with first publication rights granted to the journal.

This is an open-access article distributed under the terms and conditions of the Creative Commons Attribution license (<http://creativecommons.org/licenses/by/4.0/>).